LONG TERM *MICROPARTICLE* IMPACT FLUXES ON LDEF DETERMINED FROM OPTICAL SURVEY OF INTERPLANETARY DUST EXPERIMENT (IDE) SENSORS

C. G. Simon[1], J. P. Oliver[2], W. J. Cooke, K. I. Downey[2]
Institute for Space Science & Technology, Gainesville FL 32609

P. C. Kassel
NASA Langley Research Center, Hampton VA 23665
Phone: (804) 864-4621 Fax: (804) 864-7607

[1]Current Address: Air Consulting and Engineering, Inc.
2106 NW 67 Place, S-4, Gainesville FL 32653
Phone: (904) 335-1889 Fax: (904) 335-1891

[2]Also University of Florida, Gainesville FL 32611

SUMMARY

Many of the IDE metal-oxide-silicon (MOS) capacitor-discharge impact sensors remained active during the entire Long Duration Exposure Facility (LDEF) mission. An optical survey of impact sites on the active surfaces of these sensors has been extended to include all sensors from the low-flux sides of LDEF (i.e. the west or trailing side, the earth end, and the space end) and 5-7 active sensors from each of LDEF's high-flux sides (i.e. the east or leading side, the south side, and the north side). This survey was facilitated by the presence of a relatively large (>50 μm diameter) optical signature associated with each impact site on the active sensor surfaces. Of the ~4700 impacts in the optical survey data set, 84% were from particles in the 0.5 to 3 μm size range. An estimate of the total number of hypervelocity impacts on LDEF from particles >0.5 μm diameter yields a value of ~7 x 10^6. Impact feature dimensions for several dozen large craters on MOS sensors and germanium witness plates are also presented.

Impact fluxes calculated from the IDE survey data closely matched surveys of similar size impacts (≥3 μm diameter craters in Al, or marginal penetrations of a 2.4 μm thick Al foil) by other LDEF investigators. Since the first year IDE data were electronically recorded, the flux data could be divided into three long term time periods: the first year, the entire 5.8 year mission, and the intervening 4.8 years (by difference).

The IDE data show that there was an order of magnitude decrease in the long term microparticle impact flux on the trailing side of LDEF, from 1.01 to 0.098 x10^{-4}m^{-2}s^{-1}, from the first year in orbit compared to years 2-6. The long term flux on the leading edge showed an increase from 8.6 to 11.2 x10^{-4}m^{-2}s^{-1} over this same time period. (Short term flux increases up to 10,000 times the background rate were recorded on the leading side during LDEF's first year in orbit.) The overall east/west ratio was 44, but during LDEF's first year in orbit the ratio was 8.5, and during years 2-6 the ratio was 114.

Long term microparticle impact fluxes on the space end decreased from 1.12 to 0.55 x10^{-4}m^{-2}s^{-1} from the first year in orbit compared to years 2-6. The earth end showed the opposite trend with an increase from 0.16 to 0.38 x10^{-4}m^{-2}s^{-1}. Fluxes on rows 6 and 12 decreased from 6.1 to 3. 4 and 6.7 to 3.7 x10^{-4}m^{-2}s^{-1}, respectively, over the same time periods. This resulted in space/earth microparticle impact flux ratios of 7.1 during the first year and 1.5 during years 2-6, while the south/north, space/north and space/south ratios remained constant at 1.1, 0.16 and 0.17, respectively, during the entire mission.

This information indicates the possible identification of long term changes in discrete *microparticle* orbital debris component contributions to the total impact flux experienced by LDEF. A dramatic decrease in the debris population capable of striking the trailing side was detected that could possibly be attributed to the hiatus of western launch activity experienced from 1986-1989. A significant increase in the debris population that preferentially struck the leading side was also observed and could possibly be attributed to a single breakup event that occurred in September of 1986. A substantial increase in the

microparticle debris population that struck the earth end of LDEF, but not the space end, was also detected and could possibly be the result of a single breakup event at low altitude.

These results point to the importance of including discrete orbital debris component contribution changes in flux models in order to achieve accurate predictions of the microparticle environment that a particular spacecraft will experience in earth orbit. The only reliable, verified empirical measurements of these changes are reported in this paper. Further time-resolved *in-situ* measurements of these debris populations are needed to accurately assess model predictions and mitigation practices.

INTRODUCTION

The MOS capacitor discharge impact sensors of the Interplanetary Dust Experiment provided a unique opportunity for measuring the short term and long term time-resolved flux of small microparticles that impacted LDEF during its 5.8 year long mission. We have reported these data in several papers (Refs. 1-7) that address different aspects of the microparticle environment in low Earth orbit (LEO). In this paper we report further results of an optical survey of impacts on IDE sensors that remained active during the entire LDEF mission.

Two different sensitivity MOS sensors made up the IDE experiment. The sensitivity of the detectors is proportional to the thickness of a thermally grown layer of SiO_2 on top of a 250 μm thick, 51 mm diameter Boron-doped Si wafer substrate. The higher sensitivity detectors (0.4 μm thick dielectric, sensitive to ~0.2 μm and larger hypervelocity particle impacts) drained their batteries during the longer-than-planned LDEF mission. However, the low sensitivity IDE detectors (1.0 μm thick dielectric, sensitive to ~0.5 μm and larger hypervelocity particle impacts) remained powered during the entire mission, except for those incapacitated by large hypervelocity impacts.

The first year, time-resolved IDE data are re-presented in this paper in three separate categories: (1) Multiple Orbit Events (MOES), (2) Spikes, and (3) Background. These are described briefly with the tabulated results. More detailed descriptions of these categories, along with examples, can be found in Refs. 6 and 7.

Details of the optical survey procedures were previously published (Ref. 5). Briefly, the IDE sensors have the unique characteristic (among LDEF surfaces) of producing a clearly visible 50 μm diameter "discharge zone" around microparticle impact sites. This zone is formed by the evaporation of the 0.1 μm thick surface layer of aluminum (the top electrode) caused by heat from the electrical discharge of the MOS capacitor when struck by a particle with sufficient energy to breakdown the silicon dioxide insulator and "trigger" the sensor. The electrical discharge spark also creates a central crater with a diameter of ~10 μm. Particles >3-4 μm in size are large enough to form a spall-zone larger than the 10 μm "spark" crater, but impacts from smaller particles that triggered the sensors always resulted in a 10 μm central crater. These characteristics made it possible to quickly scan large areas of even low impact flux surfaces on LDEF (trailing side, space and earth ends) using optical microscopy. Pre- and post-flight photographs of each sensor provided a record of the few discharges produced during manufacturing and pre-flight testing. Careful correlation yielded accurate counts of impact induced discharges.

Another method of determining small particle impact fluxes on large areas of LDEF was counting penetrations through thin foils. The Multiple Abrasion Package (MAP) experiment consisted of large areas of thin aluminum and brass foils dedicated to this purpose (Ref. 8). The MAP foils were mounted adjacent to the IDE sensor arrays on 5 of the 6 orthogonal sides of LDEF (earth end excluded). After retrieval, the foils were back lighted and all penetrations counted. After additional optical and electron microscopic examination and correction for interferences (secondary impacts and non-impact induced pinholes) data from the MAP foils and from witness plates/foils of the FRECOPA experiment (Ref. 9) were plotted in smoothed flux curves (Refs. 10, 11). Although the MAP foils did not provide any level of time resolution, they did provide an excellent independent record of the microparticle impact flux for the entire 5.8 year LDEF mission which closely matched the IDE results for the same time period.

RESULTS AND DISCUSSION

Impact crater morphologies

Crater size data are presented for those interested in the material response of the MOS structure and single crystal germanium (Ge) to hypervelocity impacts. Complete optical survey results for the MOS sensors are appended to the end of this report (Table 1A). Tabulated crater size classification and measurement data are incomplete since these parameters were not part of the initial goals of the survey, but were added after the survey was underway. Results of an optical survey of two 250 μm thick, 25 mm diameter single-crystal Ge witness plates mounted on LDEF tray B-12 (north side) were previously reported (Ref. 12) and are presented here in graphical form. The passive Ge targets were also part of IDE.

Dimensions were recorded for four morphological characteristics of hypervelocity impact craters into the crystalline materials: central crater/shatter zone, inner spall zone, outer spall zone, and fracture zone. Figures 1 and 2 show plots of the measured central crater/shatter-zone maximum dimensions versus the maximum dimensions of the associated outer spalls and fracture zones of craters in the MOS and Ge surfaces, respectively. Note the convergence of the MOS data to a spall zone size equal to the central crater size at 10 μm in Fig. 1 (not predicted by the simple linear fit shown). This is consistent with the domination of the crater formation mechanism by the electrical discharge energy for small impactors (0.5-3 μm) into active MOS sensors. Above this size, the impactor energy dominated the crater formation resulting in "classic" crater/spall morphologies.

Figure 2 shows a linear response for fracture zone maximum dimensions versus central crater size, even for large features in the silicon MOS sensors. (Fracture zones were not measured for the Ge witness plate impacts.) The MOS sensors were bonded to aluminum frames with ~4 mils of silicon RTV. Apparently, shock waves from large impactors were reflected through the silicon adhesive with enough efficiency to cause fractures with the same relative dimensions as seen with smaller impactors. Figure 2 also shows that fractures that extend beyond the outer spall zones are not significant for craters smaller than ~150 μm, but are 6-7 times the maximum central crater dimension in larger impacts.

Figure 3 is a plot of central crater size versus spall zone maximum dimensions for impacts into the Ge witness plates. The largest central crater size observed was 188 μm. The near zero intercept in this plot shows the more "normal" response to small impactors of the passive crystalline Ge substrates compared to the "active" silicon MOS substrates. Observed spall zone maximum dimensions in Ge are ~6x the central crater size, while in Si they are ~3x the central crater size. This is consistent with the relative crystal lattice energies of Ge and Si.

Microparticle Impact Fluxes

Before discussing the IDE optical survey results, it is important to review a summary of the IDE time-resolved data for the first year of LDEF's orbital lifetime. These data are presented in Table 1 by detector sensitivity, location on LDEF, and impactor category (MOES, Spikes or Background). See Refs. 4 and 6 for more discussions of impactor classifications. "Spike" events were identified by visual inspection of the data file. During these events the IDE recorded tens to hundreds of impacts on the space and/or north and/or leading (east) sides of LDEF within a few minutes. These events were dominated by very small particles as evidenced by the large relative proportion of impacts from this category of particle on the high sensitivity IDE sensors compared to their low relative abundance on the low sensitivity IDE sensors.

MOES events were identified both by visual inspection of the data file and by the use of an extraction algorithm. The algorithm searched the IDE data in groups of three arrays at a time (space/north/east, space/south/east, space/south/west, space/north/west, earth/north/east, earth/south/east, earth/south/west, earth/north/west) for multiple impacts within a narrow window (34°, or ± 4.4 minutes). If two out of three adjacent orbits recorded impacts in the window, the impacts were identified as a MOES. While this method necessarily extracted some random data, in practice the MOES were very strong events which dominated the data set and limited the number of identifiable "random" impacts.

Figure 1. Central crater maximum dimensions versus spall zone maximum dimensions for impacts into the 250 µm thick IDE silicon MOS sensors.

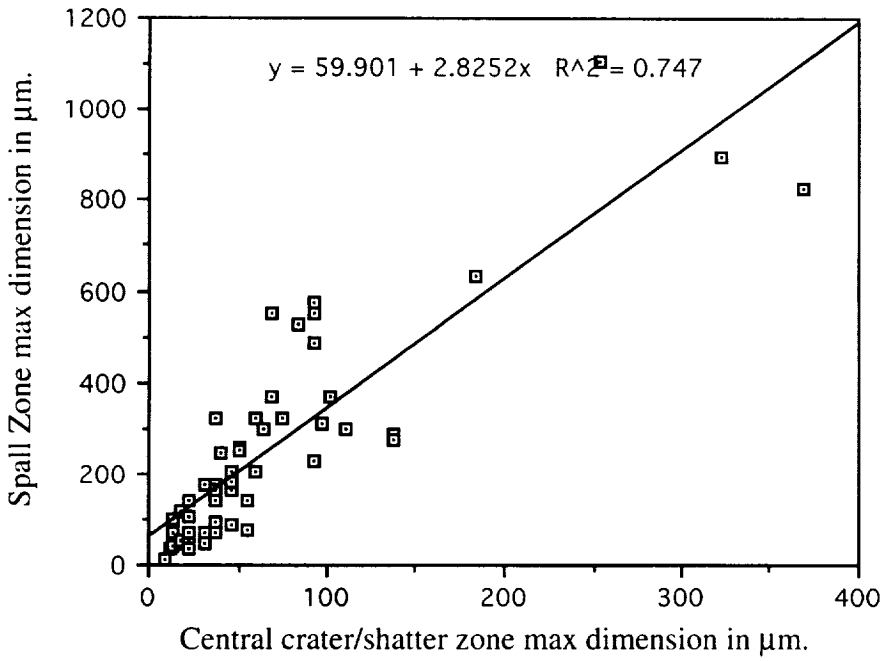

Figure 2. Central crater maximum dimensions versus fracture zone maximum dimensions for impacts into the 250µm thick IDE silicon MOS sensors.

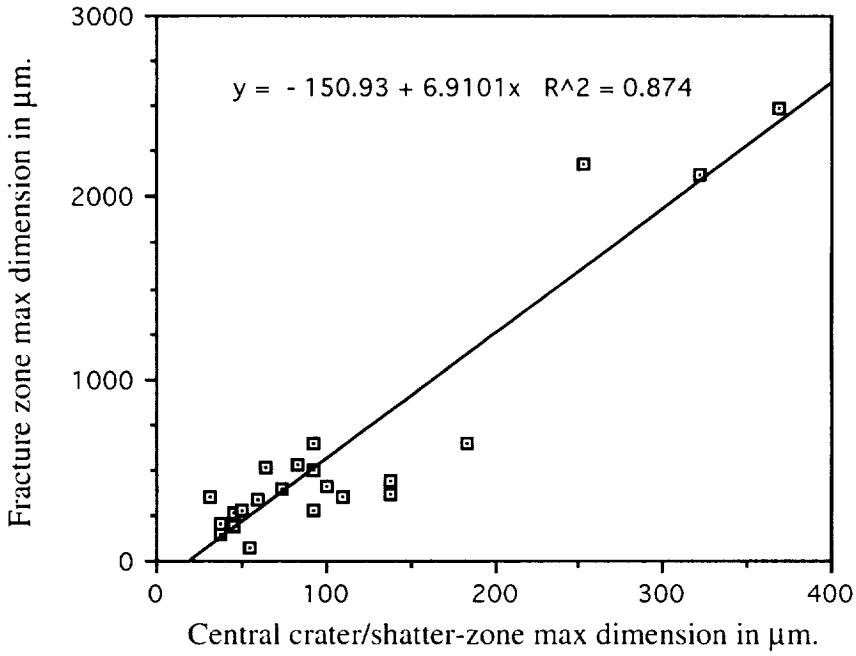

Figure 3. Central crater maximum dimensions versus spall zone maximum dimensions for impacts into 250 μm thick Ge witness plates from LDEF Row 12 (north side).

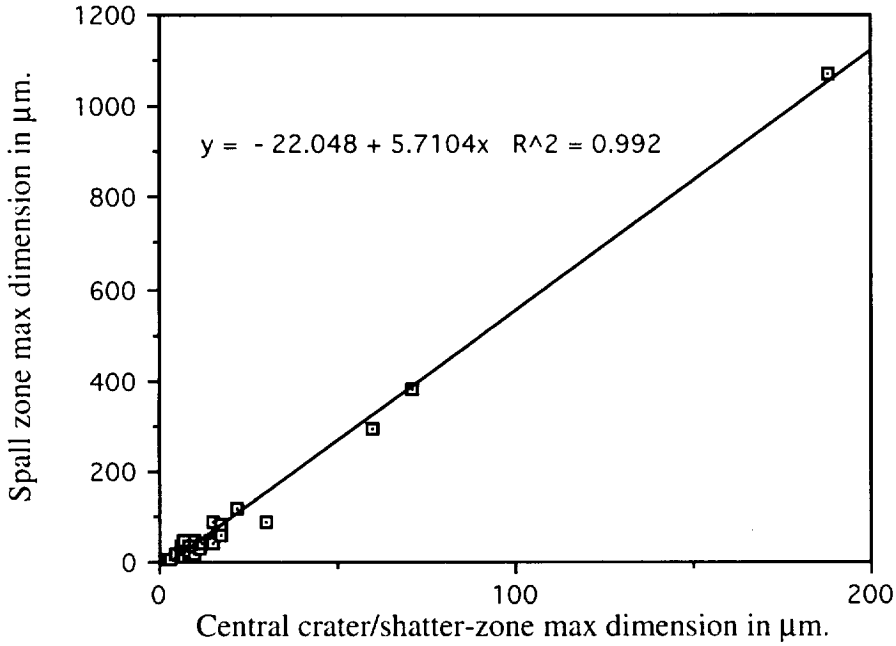

Table 1. Summary of time-resolved IDE microparticle impact data for LDEF's first year in orbit. "High" sensitivity detectors were triggered by hypervelocity particles >0.2 μm in size. "Low" sensitivity detectors were triggered by hypervelocity particles >0.5 μm in size. Results are listed in order of increasing flux.

LDEF Location	Detector Sensitivity	Impact Flux (x $10^{-4}m^{-2}s^{-1}$) Total	MOES	Spikes	Background	% of Total Flux MOES	Spikes	Background
G-10	high	0.162	0.041	0.0	0.121	25	0	75
(earth)	low	0.157	0.037	0.0	0.120	24	0	76
C-3	high	1.59	0.721	0.0	0.869	45	0	55
(west, trailing)	low	1.01	0.368	0.0	0.642	36	0	64
H-11	high	1.85	0.882	0.360	0.608	48	19	33
(space)	low	1.12	0.436	0.043	0.641	39	4	57
B-12	high	9.21	5.00	2.51	1.70	54	27	19
(north)	low	6.14	3.30	0.364	2.48	54	6	40
D-6	high	12.7	10.5	0.017	2.18	83	0.1	17
(south)	low	6.70	5.19	0.0	1.41	77	0	23
C-9	high	17.1	12.1	1.82	3.18	70	11	19
(east, leading)	low	8.61	5.59	0.182	2.84	65	2	33
Totals	high					68	11	21
	low					64	2.5	34

The IDE sensor optical survey results are summarized in Table 2 by LDEF tray location in order of increasing total-mission flux. The size range (0.5 - 3 μm) of impactors labelled "small" in the table is based on the minimum central crater diameter of 10 μm for impact induced discharges on the MOS sensors. As mentioned above, the crater formation is dominated by the electrical discharge energy for small particles. This masks all information about the impactor's size for particles smaller than ~3 μm.

The relative abundance of "small" impactors can be used to define the population of a set of particles that are significantly affected by non-gravitational forces. It is these particles that undergo rapid deviation from their parent body orbits, even when leaving with very small velocity differences (Δv). Thus, the orbits of microparticles shed from large bodies in circular orbits quickly increase in eccentricity and have very limited lifetimes. These particles can remain under the influence of the parent body for some time. For example, if they reside in shaded wake regions they will be shielded from solar pressure and aerodynamic drag effects. As a result, enhanced shedding/breakup events will release three classes of microparticles based on their leaving characteristics: (1) large Δv, (2) small Δv, and (3) "dribblers".

Shedding rate enhancements have a variety of causes, including differential thermal expansion /contraction induced vibrations and frictional wear, reaction wheel motion, solar panel motion, thruster firings, surface charge polarity shifts, plasma discharges, and hypervelocity impacts. Major sources of microparticles released during shedding include fuel residues, residual dust/dirt, and erosion products such as paint particles and thermal blanket flakes. The actual and potential particle release-rates from these sources will change drastically during an orbiting spacecraft's lifetime. These rate changes depend on a spacecraft's materials of construction and its mission operational profile, including the space environment that it experiences during its lifetime. For example, LDEF results showed that impacts into old painted surfaces released more secondary debris (spalled paint) than did impacts into "new" paint (this was due to the loss of organic binder in the paint as a result of exposure to solar ultraviolet [UV] radiation and atomic oxygen [AO]), and metal-coated hydrocarbon based foils such as Al-coated Mylar erode quickly when exposed to AO and UV, releasing bits of residual Al thin film. (See Ref. 13 for discussions of these and other examples.)

Table 2. Results of optical survey of IDE sensors that remained active during the entire LDEF mission (April, 1984-January, 1989). Scanned area = 19.6 cm^2 per sensor. Total exposure time = 2106 days. Sensors responded to iron particles >0.5 μm at velocities >2km/s in ground tests.

LDEF tray	# of sensors scanned	# sensors with craters >1mm	# "active" sensors (n) used for flux calcs.	average # of impacts per "active" sensor	std. dev. (n-1)	% of small (0.5-3 μm) impactors	impact flux $x10^{-4}m^{-2}s^{-1}$
C-3 (west)	32	4 (13%)	23	8.82	7.18 (81%)	92	0.247
G-10 (earth)	32	0 (0%)	31	12.2	6.01 (49%)	99.7	0.342
H-11(space)	22	5 (23%)	14	23.1	6.02 (26%)	77	0.647
B-12 (north)	8	5 (63%)	7	137	13.8 (10%)	85	3.84
D-6 (south)	10	3 (30%)	6	149	16.0 (11%)	78	4.17
C-9 (ram)	9	8 (89%)	5	384	30.2 (8%)	85	10.8

A summary of the long-term flux rates measured by IDE sensors and MAP foils is presented in Table 3. The MAP data are from smoothed curves generated using penetration counts (corrected for secondary impacts) from several different foil thicknesses at each location. Marginal foil penetration occurs at the point where the crater diameter is ~1.1 times the foil thickness for small impacts (Ref. 10). These data indicate that particles that will penetrate a 2.4 μm thick Al foil, or make an ~3 μm diameter crater in Al, will also trigger the low sensitivity IDE sensors. This result is consistent with ground-based calibration tests (Refs. 14, 15). The narrow range (2.34 to 2.72 μm) of equivalent foil penetration thicknesses for MAP fluxes that match IDE fluxes is particularly gratifying. These results were arrived at independently by two different groups of investigators.

The MAP data show a shift to thicker foils for the same flux value on the east side of LDEF compared to the IDE data. This indicates that the velocity enhancement effect on threshold sensitivity of the MOS sensors is not as strong as the enhanced penetration effect of Al foil due to higher velocities.

Table 3. Long-term LDEF impact flux rates measured by IDE sensors and MAP foils. Sensors responded to iron particles >0.5 μm at velocities >2km/s in ground tests. Scanned area =19.6 cm^2 per sensor. Total exposure time =2106 days. MAP data is from smoothed cumulative flux curves for marginal foil penetrations corrected for secondary impacts (Refs. 10, 11).

LDEF tray	days 1-346	days 347-2106	days 1-2106	MAP smoothed fluxes for days 1-2106	equivalent MAP Al foil thickness (μm)
C-3 (west)	1.01	0.098	0.247	0.247	2.36
G-10 (earth)	0.157	0.379	0.342	-	-
H-11(space)	1.12	0.553	0.647	0.647	2.36
B-12 (north	6.14	3.39	3.84	3.84	2.42
D-6 (south)	6.70	3.67	4.17	4.17	2.34
C-9 (east)	8.61	11.2	10.8	10.8	2.72

Flux ratios calculated from IDE and MAP results are presented in Table 4. These data illustrate the limitations of using "typical" microparticle impact flux ratios for environment effects predictions. The data also confirm the higher microparticle impact flux on the south side of LDEF compared to the north side throughout the entire mission, despite the fact that the north side was pointed 8° into the ram.

The changes in flux ratios can be used to identify possible discrete *microparticle* orbital debris component contributions to the total impact flux experienced by LDEF. Our observations show that the fluxes on the north, south and space sides decreased at about the same relative rate (by ~50%), leaving the north/space and south/space flux ratios relatively constant at ~6. These ratios should be 0.78 for meteoroid impacts alone (due to the partial earth shielding of the north and south sides). Thus, it is apparent from the overall flux ratios and from the first year, time-resolved IDE data that the microparticle impact flux on the north and south sides was dominated by orbital debris. Further, the population of debris in orbits capable of striking these surfaces apparently decreased during years 2-6. During the same time period the microparticle impact flux increased by 30% on the ram (east) surface of LDEF.

Kessler has reported on orbital debris component contributions to the observed impact flux on various sides of LDEF (Ref. 16). He showed that particles in highly inclined orbits with apogees near LDEF's would have impacted the leading (east) side of LDEF more frequently than the north or south sides. A specific example in (16) for a near circular orbit inclined 100° with an apogee of ~500 km shows a 3:1 ratio of impactors preferentially striking the leading side versus the north or south sides. An increase in the debris particle population in a highly inclined orbit such as this could produce the observed long term flux increase on the east side of LDEF while allowing for the observed long term flux decrease on the north and south sides. We note that an anti-satellite test took place in September of 1985 (vehicle designation P-78) at an altitude of ~500 km and resulted in a drastic increase in the debris population in orbits inclined ~100° (Ref. 17).

The general hiatus in western launch activities caused by the loss of several vehicles in 1986 had to result in a lower replenishment rate for the population of microparticles in 7° and 28° inclined orbits. This could account for the general lower activity on the north and south sides of LDEF. Since Kessler also showed in (16) that orbital debris particles in elliptical orbits with inclinations of ~5-40°could strike the west side of LDEF (with a peak contribution at LDEF's orbit of 28.5°), this population must also have been drastically reduced during the 1986-1990 time period. The reduction of microparticles released by western launch activities could also account for this observation.

A further observation of the time-resolved IDE data showed that ~40% of the impacts recorded by the low sensitivity detectors occurred over a relatively narrow section of LDEF's orbit (± 30° for the whole mission) centered at ~20° west with respect to the LDEF-Sun angle. (Most of these impacts were identified by the extraction algorithm as belonging to an extended MOES event. See Table 1.) These

events were first thought to be a ß-meteoroid signature, but the space end sensors showed no sign of this signature. In addition, the flux on the west side dropped by an order of magnitude from the first year to years 2-6. We also noted that the west panel average impact rate during the first year was relatively constant. Thus, we are left with the conclusion that this sun-synchronous component contribution must have decreased drastically during years 2-6 and that it could be attributed to a special case of an orbital debris MOES.

A substantial increase in the microparticle debris population that struck the earth end of LDEF (all small particles) but not the space end could possibly be the result of a single breakup event at low altitude. Such an event occurred in September of 1986 when a Delta upper stage in a 23° orbit was struck by a smaller sensor package (the Delta's payload) in a 39° orbit (Ref. 17). The intercept took place at 220 km altitude and should have produced a large outward component of microparticle debris.

Table 4. Long-term LDEF impact flux ratios measured by IDE sensors and MAP foils. These data are for impactors that would create 3 µm diameter or larger craters in an aluminum surface, or penetrate a 2.5 µm thick Al foil.

LDEF tray ratio	days 1-346	days 347-2106	days 1-2106	MAP smoothed data for days 1-2106
H-11/G-10 (space/earth)	7.13	1.46	1.89	-
H-11/C-3 (space/west)	1.11	5.64	2.62	2.87
H-11/D-6 (space/south)	0.167	0.151	0.155	0.146
H-11/B-12 (space/north)	0.182	0.163	0.168	0.166
D-6/B-12 (south/north)	1.09	1.08	1.09	1.13
C-9/C-3 (east/west)	8.52	114	43.6	58.8
C-9/D-6 (east/south)	1.29	3.05	2.58	3.00
C-9/B-12 (east/north)	1.40	3.30	2.80	3.39

CONCLUSIONS

There are several important conclusions that can be drawn from this study. First, the temporal anisotropy of the *microparticle* environment experienced by LDEF extended throughout its orbital lifetime. This has serious implications on environment predictions that rely on isotropic long term flux and flux ratio assumptions, and points to the importance of including discrete orbital debris component contribution changes in these models. Further time-resolved *in-situ* measurements of these debris populations are needed to accurately assess model predictions and mitigation practices.

Second, the IDE experiment proved that most encounters with manmade particles occur with an orbital beat frequency that indicates repeated intersections with streams of orbiting particles shed from larger orbiting objects (Refs. 2-4, 6, 7). These particles are typically very small, submicron to a few microns, and account for ~2/3 of the IDE impacts during the first year. There is no reason to assume that this situation changed during years 2-6. This is also consistent with the 84% of small (0.5 to 3 µm) particle impacts on IDE sensors observed in the optical survey.

At least two other investigators have detected similar multiple-orbit encounters on different missions since the IDE data were first reported (Refs. 18, 19). It is apparent that each spacecraft's local orbital environment will be subject to a different microparticle impact regime based on interactions with the manmade particle environment of the day. Because the particles are small, they are not expected to stay in orbit for long due to perturbation by non-gravitational forces. Thus we are left with the conclusion that for multiple orbit intersections that lasted days to weeks, there must have been a continuous emission source for these particles, such as a satellite shedding paint particles and/or other materials.

All of this leads to the conclusion that changes in the manmade microparticle population that interacted with LDEF were the major reasons for the observed changes in long term *microparticle* impact fluxes. Limited chemical analysis of impact sites on IDE sensors supports this conclusion (Ref. 20). Approximately 1/3 of the sites examined on the space and west side sensors were from manmade microparticles, mostly paint. This is a significantly higher proportion than expected, but is statistically consistent with the flux data.

A third important result is a practical lesson learned in measuring microparticle impact fluxes on surfaces that have been exposed to a very low impact-flux environment, namely that inspections of small areas can lead to radically different flux values due to the statistical uncertainty of the small data set. The IDE sensors on the Earth end and trailing side of LDEF averaged ~10 impacts per sensor, but the range of values for the number of impacts found on individual 20 cm^2 sensors was 1 to 26. We recommend that several hundred cm^2 be carefully examined when determining flux rates based on impact feature densities in the range of one impact per cm^2.

A third conclusion resulting from this study was the utility of careful pre-flight photographic documentation of flight hardware that will eventually be returned for close examination. The pre- and post-flight photographic archive of IDE sensors allowed the long term impact count to be determined with a high degree of accuracy, and identified many pre-flight contaminants that were still in place after retrieval. New contaminants were also easily identified. This situation provides an excellent opportunity for the study of contamination and its effects. All of these photographs are electronically archived with the rest of the IDE data (available on CD), and physically archived along with the IDE hardware at NASA/LaRC.

ACKNOWLEDGEMENTS

This study was supported by NASA grant NAG-1218. The authors gratefully acknowledge the helpful discussions and reviews of this work provided by Don Kessler and Don Humes.

REFERENCES

1. S. F. Singer, J. E. Stanley, *et al.*, "First Spatio-Temporal Results from the LDEF Interplanetary Dust Experiment", Advances in Space Research 11, (12) pp. 115-122, (1991).

2. J. D. Mulholland & J. L. Weinberg, "IDE Data Identifies Orbital Cloud", LDEF Spacecraft Environmental Effects Newsletter 2, #1, 15 March (1991).

3. J. D. Mulholland, S. F. Singer, *et al.*, "IDE Spatio-Temporal Impact Fluxes and High Time-Resolution Studies of Multi-Impact Events and Long-Lived Debris Clouds", LDEF-69 Months in Space: First Post Retrieval Symposium, *NASA CP 3134*, pp. 517-527 (1992).

4. J.P. Oliver, J.L. Weinberg, S.F. Singer, C.G. Simon, W.J. Wortman, W.J. Cooke, J.D. Mulholland and P.C. Kassel, "Estimation of Debris Cloud Temporal Characteristics and Orbital Elements", Proceedings of the IAF/COSPAR World Congress, W. Flury, ed., Pergamon, (1993).

5. C.G. Simon, J.D. Mulholland, J.P. Oliver, W.J. Cooke, and P.C. Kassel, "Long-term Microparticle flux Variability Indicated by Comparison of Interplanetary Dust Experiment (IDE) Timed Impacts for LDEF's First Year in Orbit with Impact Data for the Entire 5.77 Year Orbital Lifetime", LDEF-69 Months in Space: Second Post Retrieval Symposium, *NASA CP 3194*, pp. 393-704 (1993).

6. J.P. Oliver, S.F. Singer, J.L. Weinberg, C.G. Simon, W.J. Cooke, W.H. Kinard, P.C. Kassel, J.D. Mulholland and W.J. Wortman, "LDEF Interplanetary Dust Experiment (IDE) Results", LDEF-69 Months in Space: Third Post Retrieval Symposium, *NASA CP-3275* (1995).

7. William J. Cooke, John P. Oliver and Charles G. Simon, "The Orbital Characteristics of Debris Particle Rings as Derived from IDE Observations of Multiple Orbit Intersections with LDEF", LDEF-69 Months in Space: Third Post Retrieval Symposium, *NASA CP-3275* (1995).

8. J.A.M. McDonnell and T.J. Stevenson, "Hypervelocity Impact Microfoil Perforations in the LEO Space Environment (LDEF, MAP AO 023 Experiment)", LDEF-69 Months in Space: First Post Retrieval Symposium, *NASA CP 3134*, pp. 443-458 (1992).

9. J.C. Mandeville and J. Borg, "Study of Cosmic Dust Particles On Board LDEF, The FRECOPA Experiments AO138-1 and AO138-2", LDEF-69 Months in Space: First Post Retrieval Symposium, *NASA CP 3134*, pp. 419-434 (1992).

10. D.H. Niblett, S. Mullen, M.J. Neish and J.A.M. McDonnell, "Comparison of Flux Data Deduced from Observed Impacts on LDEF with Predictions from Meteoroid and Debris Models", First European Conference on Space Debris, April 5-7, Darmstadt, Germany, *ESA SD-01*, pp. 165-170 (1993).

11. J.A.M1010. McDonnell, et al., "The Near Earth Space Impact Environment - An LDEF Overview", Proceedings of the IAF/COSPAR World Congress, W. Flury, ed., Pergamon, (1993).

12. C.G. Simon, J.L. Hunter, D.P. Griffis and J.J. Wortman, "Ion microprobe elemental analysis of impact features on Interplanetary Dust Experiment sensor surfaces", LDEF-69 Months in Space: First Post Retrieval Symposium, *NASA CP 3134*, pp. 529-548 (1992).

13. A.F. Whitaker and J. Gregory, eds., "LDEF Materials Results for Spacecraft Applications", *NASA CP 3257* (1994).

14. P.C. Kassel, "Characteristics of Capacitor-Type Micrometeoroid Flux Detectors When Impacted With Simulated Micrometeoroids", *NASA TN D-7359* (1973).

15. J.J. Wortman and P.C. Kassel, "Metal-Oxide-Silicon Capacitor Detectors for Measuring Micrometeoroid and Space Debris Flux" (submitted to Journal of Spacecraft and Rockets, 1994).

16. D. Kessler, "Origin of Orbital Debris Impacts on LDEF's Trailing Surfaces", LDEF-69 Months in Space: Second Post Retrieval Symposium, *NASA CP 3194*, pp. 585-593 (1993).

17. D.J. Nauer, "History of On-orbit satellite Fragmentations", 7th ed., Teledyne-Brown Technical Report CS93-LKD-018, July (1993).

18. C.R. Maag, W.G. Tanner, T.J. Stevenson, J. Borg, J.-P. Bibring, W.M. Alexander and A.J. Maag, "Intact capture of hypervelocity impact particles and ejecta", First European Conference on Space Debris, April 5-7, Darmstadt, Germany, *ESA SD-01*, pp. 125-130 (1993).

19. J. Edelman, ed., "Summary: Second International Space Forum in Toronto", Space Flight Environment International Engineering Newsletter, Vol. 5, No. 2, p. 10 (May-June, 1994).

20. C.G. Simon, J.L. Hunter, D.P. Griffis, V. Misra, D.A. Ricks, J.J. Wortman, and D.E. Brownlee, "Elemental analyses of hypervelocity microparticle impact sites on Interplanetary Dust Experiment sensor surfaces." LDEF-69 Months in Space: Second Post Retrieval Symposium, *NASA CP-3194*, pp. 677-692 (1993).

Table 1A. Optical survey results for IDE low sensitivity MOS sensors listed by LDEF location in order of increasing impact flux. Sensor dielectric thickness =1.0 μm; active surface area =19.6 cm^2/sensor; total exposure time =2106 days. In ground tests, these sensors responded to iron particles > 0.5 μm diameter at velocities >2 km/s (Refs. 14, 15). LDEF data showed that the sensors responded to any impactor that would produce craters in aluminum >3 μm diameter, or penetrate a 2.4 μm thick Al foil. Dimensions for craters are listed in microns (±5) as central-crater-dia/outer-spall-max-dimension/fracture-zone-max-dimension. A question mark (?) indicates that a measurement was not made; a dash (-) indicates that the feature was not present or not discernible. Sensors that gave all indications of having been active during the entire LDEF mission were used to calculate impact fluxes and are marked with an asterisk (*).

C = hypervelocity impact crater with no visual evidence of associated discharge.
d = impact induced discharge, nominal central crater (<14 μm diameter).
D = impact induced discharge, central crater/inner spall 14 - 20 μm diameter.
D = impact induced discharge, central crater/inner spall 20-50 μm diameter.
D = impact induced discharge, central crater/inner spall >50 μm diameter. $\mathbf{D_{tot}}$ = all impact discharges.

Sensor Number	C	d	D	D	*D*	D_{tot}	D_{tot}+C
Tray C-3 ("west", or "trailing" side)							
*1180	0	7	0	0	60/322/?	*7	7
*1182	0	9	0	0	0	*9	9
1183	?/20/? ?/~400/?	9	0	0	0	9	11
1191(short)	?/~5300/45000	12	0	0	0	12	13
*1192	0	6	0	0	0	*6	6
*1208	0	6	0	0	?/~100/? ?/~100/?	*8	8
*1213	0	7	0	0	0	*7	7
1224	1	6	0	0	?/~500/?	6	7
1237	64/299/506	3	0	0	-/69/106 368/828/2484	5	6
*1248	0	7	0	0	322/897/2116	*8	8
*1249	0	4	0	0	0	*4	4
*1268	0	2	0	0	0	*2	2
*1271	0	5	0	14/69/-	46/184/-	*7	7
*1276	0	4	0	0	37/69/207	*5	5
*1294	0	4	0	0	0	*4	4
*1300	0	24	-/17/-	0	37/140/149	*26	26
*1305	0	?	?	?	0	*12	12
*1310	0	26	0	0	0	*26	26
*1312	0	?	?	?	0	*5	5
*1320	0	?	?	?	0	*6	6
1335(short)	37/322/-	0	0		0	0	1
*1336	0	?	?	?	?	*8	8
*1342	0	2	0	41/248/-	0	*3	3
*1356	0	4	0	-/28/-	0	*5	5
1359	7(secondaries)	18	0	-/30/-	0	19	26
1361	1	9	0	0	0	9	10
*1365	0	4	0	0	0	*4	4
*1382	0	7	-/20/-	-/30/-	1	*10	10
*1387	0	5	0	0	0	*5	5
1395(short)	0	11	0	0	0	11	11
*1401	0	25	0	0	74/322/391	*26	26
1403	253/1104/2185	0	0	23/106/-	0	2	3

Table 1A (continued)

Sensor Number	C	d	D	D	*D*	D_{tot}	D_{tot}+C

NOTE: On C-3, 4 sensors out of 32 have craters >1mm. Sensor 1191 was cracked in half by a large impact. *n=23, mean = 8.82±7.18. 92% of impacts were from hypervelocity microparticles ~0.5 to 3 μm diameter.

Tray G-10 (earth facing side)

*1172	0	21	0	0	0	*21	21
*1173	0	1	0	0	0	*1	1
*1174	0	1	0	0	0	*1	1
*1177	0	5	0	0	0	*5	5
*1210	0	10	0	0	0	*10	10
*1218	0	6	0	0	0	*6	6
*1219	0	16	0	0	0	*16	16
*1220	0	12	0	0	0	*12	12
*1232	0	14	0	0	0	*14	14
*1234	0	15	0	0	0	*15	15
*1239	0	12	0	0	0	*12	12
*1241	0	7	0	0	0	*7	7
*1279	0	6	0	0	0	*6	6
*1280	0	14	0	0	0	*14	14
*1282	0	9	0	0	0	*9	
*1284	0	14	0	0	0	*14*	14
*1290	0	9	0	0	0	*9	9
*1291	0	13	-/18/-	0	0	*14	14
*1297	0	8	0	0	0	*9	9
*1304	0	16	0	0	0	*16	16
*1322	0	7	0	0	0	*7	7
1323(short)	0	1	1	0	0	2	2
*1326	0	2	0	0	0	*2	2
*1349	0	19	0	0	0	*19	19
*1350	0	14	0	0	0	*14	14
*1351	0	20	0	0	0	*20	20
*1360	0	19	0	0	0	*19	19
*1378	0	19	0	0	0	*19	19
*1381	0	23	0	0	0	*23	23
*1386	0	10	0	0	0	*10	10
*1390	0	16	0	0	0	*16	16
*1391	0	19	0	0	0	*19	19

NOTE: On G-10 sensors there were no large impacts. Sensors 1234, 1291, 1297 and 1381 have Al debris spray droplets from distant impacts. No impacts into sensor frames were noted. Sensor 1297 had a piece of Fe/Si rich meteorite residue contained in an Al debris spray droplet (apparently from an impact into the LDEF walking beam). Sensors 1172 and 1297 have suspected wastewater droplet residues. *n = 31, mean = 12.2± 6.01. 99.7% of impacts were from particles 0.5 - 3 μm in size.

Table 1A (continued)

Sensor Number	C	d	D	D	D	D_{tot}	D_{tot}+C
Tray H-11 (space facing side)							
*1193	0	14	0	37x55/138/-	138/290/370 138x184/634/644 101/370/414	*18	18
*1194	0	16	0	18x32/69/- 23x55/74/74 32/175/359 37/161/- 46/88/- 46/99/299	92x110/299/350	*23	23
*1195	0	10	-/14/- -/18/- -/18/-	-/23/- 37/175/- 14/101/-	50/253/-	*17	17
1203	83/529/529	14	18/115/-	23/37/- 23/41/- 46/207/- 50/258/276	0	19	20
*1205	0	24	-/18/-	-/23x28/- 32/46/- 41/-/-	92/575/644	*29	29
1226 (short)	11 (see size listings to right)	1	9/14/-.(C) 12/35/- (C) 14/41/- (C)	23/55/- (C) 23/69/- (C) 23/138/- (C) 37/92/207 (C)	60/207/331 (C) 92/230/276 (C) 97/313/- (C) 92x138/276/437 (C)	1	12
*1244	0	15	18/46/- 18/55/-	23/-/- 23/69/- 37/175/-	69/368/- 69/552/- 92/552/-	*23	23
*1254	0	13	-/18/- 14/37/- 18/115/-	-/23/- -/23/- -/32/- 46/166/265	92/483/493	*21	21
*1255	0	18	0	0	1	*19	19
1261	1	15	1	3	2	21	22
1296(short)	0	7	2	0	3	12	12
*1303	0	27	3	2	1	*33	33
*1313	0	21	3	1	1	*26	26
*1340	0	28	0	1	6	*35	35
*1343	0	12	2	0	1	*15	15
*1370	0	16	2	0	0	*18	18
*1371	0	18	2	0	1	*21	21
1372	2	21	3	1	0	25	27
*1379	0	19	2	1	4	*26	26
1385 (short)	2	13	2	3	0	18	20
1399	1	21	1	0	0	21	23
1400	2	15	1	0	2	18	20

Table 1A (continued)

Sensor Number	C	d	D	$\underline{D}$	*D*	D_{tot}	D_{tot}+C

NOTE: On H-11, 5 sensors out of 22 have craters >1mm; sensor 1385 has 2 large craters. Sensors 1203, 1226, 1340, 1379, and 1400 have Al debris sprays from impacts into their frames. Sensors 1195 and 1226 have suspected wastewater droplet residues. *n = 14, mean = 23.1±6.0. 77% of impacts were from particles 0.5 - 3 μm in size.

Tray B-12 ("north" side)

*1175	0	110	28	6	0	*144	144
*1202	0	104	11	13	0	*128	128
1217	5	44	6	2	3	55	60
*1278	0	107	6	2	5	*120	120
*1298	(1)	-	-	-	-	*132	133
*1324	0	145	4	3	3	*155	155
*1352	0	114	5	5	2	*126	126
*1384	0	121	26	6	-	*153	153

NOTE: On B-12, 5 sensors out of 8 examined have craters>1mm. Sensor 1298 has 2 large craters. *n = 7, mean = 137±13.8. 85% of impacts were from particles 0.5 - 3 μm in size.

Tray D-6 ("south "side)

*1186	0	100	20	10	8	*138	138
1187(short)	30	?	?	?	22	52	
*1190	0	122	22	18	0	*162	162
*1212	0	116	20	6	2	*144	144
1225(short)	15	?	?	?	82	97	
1252(short)	14	?	?	?	37	51	
1253	4	64	12	11	9	96	100
*1263	1	130	21	7	0	*158	159
*1311	0	137	23	3	2	*165	165
*1314	0	89	29	6	0	*124	124

NOTE: On D-6, 3 sensors out of 10 examined have craters >1mm. Sensor 1225 has a 6 mm hexagon crack/spall around a large crater. *n = 6, mean = 149±16.0. 78% of impacts were from particles 0.5 - 3 μm in size.

Tray C-9 ("east" or "leading" side)

*1176	0	?	?	?	?	*357	357
1293	10	?	?	?	?	200	210
1333	11	121	13	11	6	151	162
1334(short)	53	?	?	?	?	152	205
*1355	0	321	39	21	7	*388	388
*1383	0	339	18	?	10	*367	367
*1396	0	356	46	22	10	*434	434
*1406	0	305	47	12	8	*373	373

NOTE: On C-9, 8 sensors out of 8 examined have craters >1mm. One sensor has 3 large craters. Sensor 1355 has a large debris spray from an impact into its aluminum frame. Sensor 1293 has a suspected wastewater droplet residue. *n=5, mean = 384±30.2. 85% of impacts were from particles 0.5 - 3 μm in size.